BMC Medical Imaging

RESEARCH

Open Access

The combination of focal breast edema and adjacent vessel sign to assess the behavior of mass-type invasive ductal carcinoma

Juanjuan Hu[1†], Junli Ke[1], Shufeng Xu[1], Lei Pei[1], Lulu Cao[2], Huanhao Zhou[3] and Xisong Zhu[1*]

Abstract

Background The objective of this study was to investigate the association between focal breast edema (FBE) and adjacent vessel sign (AVS) with tumor size, histologic grade, lymphovascular invasion, axillary lymph node status, Ki-67 index, and molecular subtype in breast cancer. These findings have provided valuable insights into the biological characteristics and prognosis of mass-type invasive ductal carcinoma (M-IDC).

Methods We retrospectively included patients with M-IDC between January 2016 and December 2021. FBE was evaluated using T2-weighted sequence. AVS was assessed using maximum-intensity projection images obtained using early dynamic contrast-enhanced magnetic resonance imaging. The breast peritumor score (BPS) was defined as follows: BPS 1, absence of both edema and AVS; BPS 2, AVS without edema; BPS 3, AVS with peritumoral edema; BPS 4, AVS with prepectoral edema; and BPS 5, AVS with subcutaneous edema. The correlation between different BPS scores and clinicopathological variables was examined using Kendall's tau-b correlation coefficient. The DeLong test was used to compare the performances of three clinicopathological models combined with peritumoral features (FBE, AVS, and BPS) in predicting luminal A-like M-IDC.

Results In 228 patients with M-IDC, BPS was positively correlated with tumor size, histologic grade, lymphovascular invasion, axillary lymph node status, Ki-67 index, and negatively correlated with estrogen receptor expression (all $P < 0.05$). Furthermore, BPS 1 was more likely to be present in patients with luminal A-like breast cancer ($P < 0.001$). Among the three prediction models, the clinicopathological model combined with the BPS model demonstrated superior diagnostic performance for luminal A-like breast cancer.

Conclusions The BPS is a valuable, non-invasive biomarker for assessing the aggressiveness of M-IDC and can facilitate treatment planning.

Keywords Breast neoplasms, Magnetic resonance imaging, Edema, Adjacent vessel sign

[†]Juanjuan Hu is the first author.

*Correspondence:
Xisong Zhu
zhuxisong@126.com
[1]Department of Radiology, The Quzhou Affiliated Hospital of Wenzhou Medical University, Quzhou People's Hospital, 100 Minjiang Avenue, Kecheng District, Quzhou 324000, P.R. China
[2]Department of Pathology, The Quzhou Affiliated Hospital of Wenzhou Medical University, Quzhou People's Hospital, Quzhou, P.R. China
[3]Department of Breast Surgery, The Quzhou Affiliated Hospital of Wenzhou Medical University, Quzhou People's Hospital, Quzhou, P.R. China

Introduction

Breast cancer has the highest incidence among women worldwide and it is the leading cause of cancer-related mortality in women [1]. Breast magnetic resonance imaging (MRI) is widely acknowledged as the most precise diagnostic tool for screening women at high risk of breast cancer, staging breast cancer, and evaluating their response to neoadjuvant chemotherapy [2]. Compared to full-protocol MRI, abbreviated screening MRI, which includes a T2-weighted (T2WI) sequence, one precontrast sequence, and one postcontrast T1-weighted (T1WI) sequence, has been extensively studied because of its comparable sensitivity and superior specificity [3, 4]. The utilization of both T2WI and early postcontrast T1WI significantly enhances the diagnostic accuracy of breast cancer.

Several studies suggest that MRI characteristics of peritumoral tissues offer valuable insights into the biological information and prognostic outcomes associated with breast cancer [5, 6]. The presence of focal breast edema (FBE) characterized by a clear hyperintense signal compared to the ipsilateral pectoralis major, on T2WI in the same breast or adjacent to the tumor, is frequently indicative of malignancy [7]. FBE is classified as peritumoral, prepectoral, and subcutaneous [8]. Many studies have confirmed that FBE is associated with high biological aggressiveness and poor prognosis of breast cancer [9, 10]. In addition, Harada et al. [10] have established the breast edema score (BES) in 2021 to grade breast edema on T2WI sequences and proved that the BES has important guiding significance for the evaluation of progression-free and overall survival of breast cancer. The adjacent vessel sign (AVS) on early dynamic contrast-enhanced (EDCE) imaging was initially defined as the presence of a vessel (either an artery or vein) in direct proximity to or accessing a lesion [11]. The inclusion of AVS as an adjunctive prognostic factor may enhance the accuracy of predicting a poor prognosis [12].

However, the clinical significance and prognostic value of peritumoral tissues have not been fully elucidated. We have developed a breast peritumor score (BPS): BPS 1, the absence of both edema and AVS; BPS 2, AVS without edema; BPS 3, AVS with peritumoral edema; BPS 4, AVS with prepectoral edema; and BPS 5, AVS with subcutaneous edema. The purpose of this study was to investigate the correlation between BPS and clinicopathological characteristics in patients with mass-type invasive ductal carcinoma (M-IDC). The objective of our study was to utilize the BPS to provide valuable biological information for the development of personalized treatment strategies for patients with M-IDC.

Methods

Study population

This retrospective study was approved by our institutional review board and ethics committee, and the requirement for informed consent was waived. This study conducted a retrospective analysis of the clinical pathology and imaging data of female patients with breast cancer between January 2016 and December 2021. To avoid interference from normal fibroglandular tissue or fat tissue within the non-mass enhancement lesions, we included only mass lesions. According to the 2013 edition of the American College of Radiology Breast Imaging Reporting and Data System, a mass is a three dimensional, space-occupying structure with a convex-outward contour [13]. A total of 355 women with invasive ductal carcinoma on breast MRI were identified using the hospital case system and Picture Archiving and Communication System. Among them, 21 underwent puncture biopsy or neoadjuvant therapy before the MRI examination, 52 showed non-mass enhancement, 36 showed multiple unilateral or bilateral masses, and 18 showed positive surgical margins or ductal carcinoma in situ around the lesion, and were excluded. A total of 228 patients were included in the study. An overview of the patient selection process is shown in Fig. 1.

MRI technique

All MRI examinations were performed using a 1.5-T superconductive MRI scanner (Achieva, Philips Healthcare) with a 4-channel body array coil. The scanning parameters were as follows: (1) conventional axial T1W-TSE sequence: TR 439 ms, TE 9 ms, slice thickness 3.5 mm; (2) transection T2W-SPAIR (SPectral Attenuated Inversion Recovery) sequence: TR 3740 ms, TE 60 ms, 3.5 mm thick; (3) sagittal T2W-SPAIR sequence: TR 4255 ms, TE 74 ms, thick 4.0 mm; (4) Dyn-eTHRIVE sequence was used to perform axial fat-suppressed T1-weighted gradient-echo dynamic enhanced scan: TR 6.9 ms, TE 3.4 ms, 1 mm thick, matrix 300×300, turning angle of 10°, a total of nine phases, scan time was 8 min 15 s, the maximum-intensity projection (MIP) images were obtained by subtraction.

MRI evaluation

Two doctors, each with over five years of experience in breast MRI diagnosis, independently reviewed the images without knowledge of the patients' pathological results. If there was a discrepancy between the two radiologists, the final decision was made by a chief physician specializing in breast MRI diagnosis with over 20 years of experience. Interobserver agreement was tested using kappa statistics.

The parameters assessed using MRI included tumor size, FBE on T2WI, and the adjacent vessel sign (AVS) on

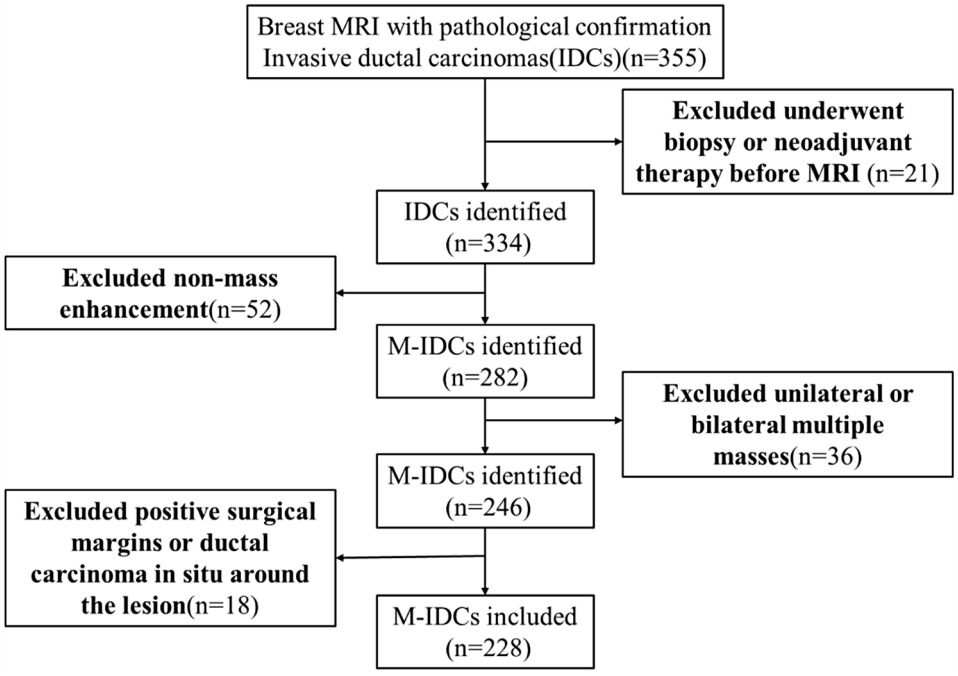

Fig. 1 Study flowchart of participant selection

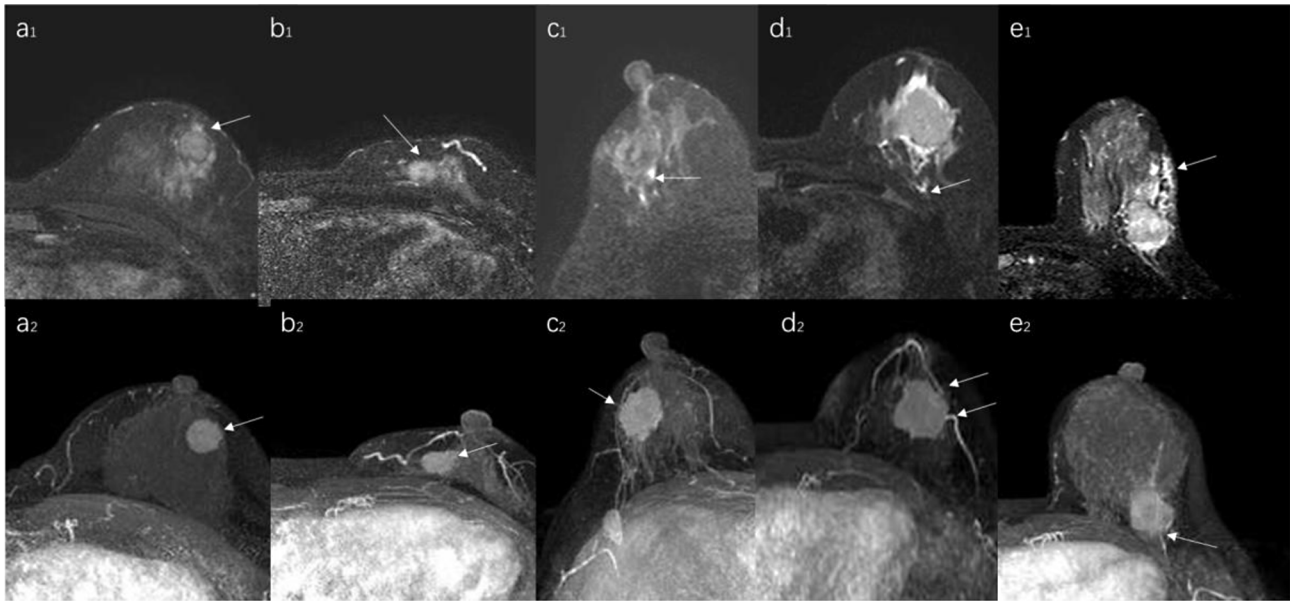

Fig. 2 Example of breast peritumor score (BPS) on MRI. a1–a2 BPS1: A left invasive ductal carcinoma with histological grade II. There was no high signal intensity (no edema) around the tumor at axial fat-suppressed T2-weighted imaging (T2WI), and axial fat-suppressed T1-weighted EDCE (the second MIP) showed no AVS. b1–b2 BPS2: A left invasive ductal carcinoma with histological grade II. There was no edema at axial fat-suppressed T2WI, and EDCE-MIP showed a vessel in contact with a lesion (AVS). c1–c2 BPS3: A right invasive ductal carcinoma with histological grade II. axial fat-suppressed T2WI showed a linear-shaped hyperintensity (peritumoral edema) around the tumor, and EDCE-MIP showed several vessels in contact with a lesion or entering it (AVS). d1–d2 BPS4: A left invasive ductal carcinoma with histological grade III. axial fat-suppressed T2WI showed a band-shaped hyperintensity extended to the anterior space of pectoralis major muscle (prepectoral edema), and EDCE-MIP showed several vessels in contact with a lesion or entering it (AVS). e1–e2 BPS5: A left invasive ductal carcinoma with histological grade III. axial fat-suppressed T2WI showed the obvious hyperintensity of skin and subcutaneous fat with skin thickening (subcutaneous edema), and EDCE-MIP showed a vessel entering a lesion (AVS)

the MIP of EDCE. Tumor size was determined based on the maximum diameter observed in the MRI enhancement sequence, and the final value was calculated as the average of measurements conducted by two physicians. FBE was assessed using T2W-SPAIR and categorized as the absence of edema, peritumoral edema, prepectoral edema, or subcutaneous edema. The presence of peritumoral edema was determined by identifying a distinct, localized region exhibiting high-intensity signals (in comparison to the ipsilateral pectoralis major), resembling aqueous characteristics on T2WI. Furthermore, the extent of edema surrounding the tumor did not surpass its borders and no cyst wall was observed on EDCE. The presence of prepectoral edema was ascertained through visual examination of an enlarged region displaying intense water-like signals characterized by a linear or ribbon-like extension close to the pectoralis major muscle. The presence of subcutaneous edema was determined by the conspicuous high-signal-intensity area of skin and skin thickening on T2WI. When a tumor was located directly beneath the skin and accompanied by localized region subcutaneous edema, it was classified as peritumoral edema. The occurrence of three types of edema, including peritumoral edema, prepectoral edema, and subcutaneous edema at the same time, was mainly relatively high grade according to the breast edema score. AVS was defined as the presence of a vessel (either an artery or vein) in direct proximity to or accessing a lesion. The presence of AVS was ascertained through the second MIP image, which was meticulously scrutinized through 360° rotations in three directions to comprehensively assess the surface and vasculature of the mass. The combination of FBE and AVS was used to establish the BPS, which was defined as follows: BPS 1, the absence of both edema and AVS (Fig. 2a1-a2), BPS 2, AVS without edema (Fig. 2b1-b2), BPS 3, AVS with peritumoral edema (Fig. 2c1-c2), BPS 4, AVS with prepectoral edema (Fig. 2d1-d2), and BPS 5, AVS with subcutaneous edema (Fig. 2e1-e2).

Pathologic analysis

The clinical and pathological characteristics of all patients were collected for analysis, including age, tumor size, histological grade, lymphovascular invasion (LVI) status, axillary lymph node (ALN) status, estrogen receptor (ER) expression, human epidermal growth factor receptor (HER2) status, and Ki-67 index. According to the fifth edition of the World Health Organization classification of breast tumors in 2019 [14], immunohistochemical detection criteria were as follows: (1)ER/progesterone receptor (PR) positive was defined as positive tumor nucleus ≥ 1%, and < 1% was ER/PR negative. (2)The HER2 positive status was defined as a HER2 expression score of (+++), while (-) and (+) indicated HER2 negative. To further validate the expression score, fluorescence in situ hybridization gene detection was performed in cases of (++), confirming the presence of HER2 amplification and classifying it as HER2 positive. (3) A threshold value of 14% Ki-67 was used to distinguish between high and low levels. Breast cancer was divided into five molecular subtypes: luminal A-like, luminal B-like (HER2-negative), luminal B-like (HER2-positive), HER2 positive (non-luminal), and triple-negative.

The construction of predictive models

The luminal A-like and non-luminal A-like subtypes were used as outcome variables. Univariate analysis was used to determine the clinicopathological factors significantly correlated with luminal A-like M-IDCs ($P < 0.05$). the peritumoral features of the three groups (FBE, AVS, and BPS) and the clinicopathological factors with statistical significance in univariate analysis were combined, and multivariate logistic regression analysis was performed separately. Therefore, this study developed three predictive models: the clinicopathological-FBE (CPF), clinicopathological-AVS (CPA), and clinicopathological-BPS (CPP) models.

Statistical analysis

The statistical analyses were conducted using SPSS software, version 25.0 (IBM Corp.), with a significance level set at $P < 0.05$. The correlation between the BPS and clinicopathological characteristics was compared between patients with M-IDC. Student's t-test for independent variables with a normal distribution and Mann-Whitney U-test for variables with a non-normal distribution were employed to conduct intergroup comparisons. Categorical variables were compared using either Pearson's chi-square test or Fisher's exact test. The association between the BPS and clinicopathological variables was investigated using Kendall's tau-b correlation coefficient. Interobserver variability was computed to assess the categorical ratings provided by the two reviewers using k-statistics.

The receiver operating characteristic curve and area under the curve (AUC) were used to evaluate the diagnostic efficacy of the model for luminal A-like and non-luminal A-like classifications. The DeLong test was used to compare statistical significance in the prediction performance of the three models, and $P < 0.05$ was considered statistically significant.

Results

Basic information of included patients

In total, 228 female patients with M-IDC were enrolled in this study. The mean age at diagnosis was (52.5 ± 8.4) years, ranging from 30 to 82 years old. The median maximum diameter of the tumor on MRI was 2.7 cm, with

a range from 0.9 cm to 5.3 cm. The study included 114 patients with and 114 without FBE; 196 patients with AVS and 32 without AVS. The combination of FBE and AVS identified BPS: out of the total of 228 lesions, 32 were classified as BPS 1, 82 as BPS 2, 89 as BPS 3, 15 as BPS 4, and 10 as BPS 5.

Breast peritumor score (BPS)

Table 1 shows the correlation between BPS and clinicopathological features in patients with M-IDC. BPS correlated with tumor size ($P<0.001$), histologic grade ($P<0.001$), LVI status ($P<0.001$), ALN status ($P=0.014$), Ki-67 index ($P<0.001$), and ER expression ($P<0.001$). In the intergroup comparison, lesions with BPS 3, 4, and 5 exhibited larger tumor sizes and higher histologic grades than those with BPS 1 and 2. Lesions with BPS 2, 3, 4, and 5 exhibited a higher Ki-67 index, LVI positivity, and prevalence of ALN involvement than those with BPS 1. Lesions with BPS 3, 4, and 5 were significantly more common and exhibited a negative ER status than those with BPS 1. BPS 1 and 2 lesions did not differ significantly in tumor size, histologic grade, or ER expression, and lesions with BPS 2 compared with BPS 1 displayed a higher Ki-67 index, LVI positivity, and prevalence of ALN involvement. BPS scores of 3, 4, and 5 did not differ significantly in any of the clinicopathological features.

Correlation analysis showed that BPS positively correlated with tumor size (Kendall's tau-b=0.454, $P<0.001$), histologic grade (Kendall's tau-b=0.403, $P<0.001$), LVI (Kendall's tau-b=0.240, $P<0.001$), ALN status (Kendall's tau-b=0.151, $P=0.01$), Ki-67 index (Kendall's tau-b=0.341, $P<0.001$), and expression of ER (Kendall's tau-b = -0.289, $P<0.001$). The ordered variable BPS showed weak to moderate correlations with tumor size, histologic grade, LVI, Ki-67 index, and expression of ER.

Interobserver agreement

An almost perfect interobserver agreement was observed for BES (k=0.805) and AVS (k=0.736).

Molecular subtype associated with Peritumoral features

Table 2 shows the correlation between molecular subtype and BPS in M-IDCs. Patients with non-luminal M-IDC (HER2-positive and triple-negative) were more inclined to present with larger tumors, AVS-positive, FBE-positive, and higher histologic grades (Fig. 3) than those with luminal A-like M-IDC (all $P<0.05$). However, BPS 1 lesions were more likely to be luminal A-like tumors ($P<0.001$)(Fig. 4).

Table 1 Correlation between breast peritumor score and clinical-pathological features in M-IDC[Mean ± SD, IQR, n (%)]

Variables	BPS					*P*
	BPS1 (*n*=32)	**BPS2 (*n*=82)**	**BPS3 (*n*=89)**	**BPS4 (*n*=15)**	**BPS5 (*n*=10)**	
Age in years	49.59 ± 7.36	51.79 ± 8.61	53.67 ± 10.85	52.20 ± 8.06	57.10 ± 7.98	0.121
Tumor size on MRI in cm	1.50(1.17–1.80)	1.90(1.50–2.30)	2.20(2.00-2.90) ◪▲	3.00(2.50–3.40) ◪▲	3.30(3.00-3.50) ◪▲	<**0.001**
Histologic grade						<**0.001**
I/II	29(90.62)	60(73.17)	35(39.33)	5(33.33)	2(20.00)	
III	3(9.38)	22(26.83)	54(60.67) ◪▲	10(66.67) ◪▲	8(80.00) ◪▲	
LVI status						<**0.001**
Negative	28(87.50)	49(59.76)	48(53.93)	5(33.33)	3(30.00)	
Positive	4(12.50)	33(40.24) ◪	41(46.07) ◪	10(66.67) ◪	7(70.00) ◪	
ALN status						**0.014**
Negative	29(90.62)	51(62.20)	57(64.04)	9(60.00)	4(40.00)	
Positive	3(9.38)	31(37.80) ◪	32(35.96) ◪	6(40.00)	6(60.00) ◪	
Ki-67 index						<**0.001**
< 14	21(65.62)	25(30.49)	9(10.11)	3(20.00)	1(10.00)	
≥ 14	11(34.38)	57(69.51) ◪	80(89.89) ◪▲	12(80.00) ◪	9(90.00)	
ER						<**0.001**
Negative	2(6.25)	22(26.83)	37(41.57) ◪	8(53.33) ◪	7(70.00) ◪	
Positive	30(93.75)	60(73.17)	52(58.43)	7(46.67)	3(30.00)	
HER2						0.686
Negative	27(84.38)	59(71.95)	66(74.16)	12(80.00)	7(70.00)	
Positive	5(15.62)	23(28.05)	23(25.84)	3(20.00)	3(30.00)	

Statistically significant *p*-values are bolded

BPS 1: absence of both edema and AVS, BPS 2:AVS without edema, BPS 3: AVS with peritumoral edema, BPS 4:AVS with prepectoral edema, BPS 5:AVS with subcutaneous edem

compare with BPS 1: ◪ $P<0.05$, compare with BPS 2: ▲ $P<0.05$

Table 2 Correlation between molecular subtype and peritumoral features in M-IDC[Mean ± SD, IQR, n (%)]

Variables	Molecular subtype					*P*
	1[a](*n* = 52)	**2[b](*n* = 70)**	**3[c](*n* = 29)**	**4[d](*n* = 29)**	**5[e](*n* = 48)**	
Age in years	53.40 ± 9.26	53.14 ± 9.90	51.52 ± 7.85	52.00 ± 9.63	51.38 ± 9.81	0.760
Tumor size on MRI in cm,	1.75(1.50–2.20)	2.30(1.72–2.75)	2.00(1.70–2.90)	2.20(1.70-3.00)	2.15(1.78–2.70)	**0.042**
AVS						<**0.001**
Negative	19(36.54) ▲,*	8(11.43) ▲	3(10.34)	1(3.45) ▲	1(2.08) ▲	
Positive	33(63.46)	62(88.57)	26(89.66)	28(96.55)	47(97.92)	
FBE						<**0.001**
Negative	40(76.92) ▲,*	33(47.14) ▲	17(58.62)	10(34.48) ▲	14(29.17) ▲	
Positive	12(23.08)	37(52.86)	12(41.38)	19(65.52)	34(70.83)	
BPS						<**0.001**
1	19(36.54) ▲,*	8(11.43) ▲	3(10.34)	1(3.45) ▲	1(2.08) ▲	
2	21(40.38)	25(35.71)	14(48.28)	9(31.03)	13(27.08)	
3	8(15.38) ▲*	30(42.86) ▲	12(41.38)	13(44.83) ▲	26(54.17) ▲	
4	3(5.77)	5(7.14)	0(0.00)	3(10.34)	4(8.33)	
5	1(1.92)	2(2.86)	0(0.00)	3(10.34)	4(8.33)	
Histologic grade						<**0.001**
I/II	50(96.15)▲▽,*	48(68.57)*	16(55.17) ◪*	9(31.03) ◪▲	8(16.67) ◪▲▽	
III	2(3.85)	22(31.43)	13(44.83)	20(68.97)	40(83.33)	
LVI status						0.571
Negative	31(59.62)	36(51.43)	18(62.07)	20(68.97)	28(58.33)	
Positive	21(40.38)	34(48.57)	11(37.93)	9(31.03)	20(41.67)	
ALN status						0.347
Negative	33(63.46)	43(61.43)	19(65.52)	24(82.76)	31(64.58)	
Positive	19(36.54)	27(38.57)	10(34.48)	5(17.24)	17(35.42)	

Statistically significant *p*-values are bolded

1[a]: Luminal A-like, 2[b]: Luminal B-like (HER2-negative), 3[c]: Luminal B-like (HER2-positive), 4[d]: HER2 positive (non-luminal), 5[e]: Triple-negative

compare with Luminal A-like: ◪P<0.05, compare with Luminal B-like (HER2-negative): ▲P<0.05, compare with Luminal B-like (HER2- positive): ▽P<0.05, compare with HER2 positive (non-luminal):*P<0.05, compare with Triple-negative: *P<0.05

Three prediction models for luminal A-like M-IDC

Univariate analysis showed that tumor size and histological grade were clinicopathological predictors of luminal A-like M-IDCs. The variables FBE, tumor size, and histological grade were included in the multivariate logistic regression analysis. Histological grade (OR = 0.05, 95%CI: 0.01–0.20, *P* < 0.001) was identified as an independent predictor, leading to the construction of the CPF model. AVS, tumor size, and histological grade were included in the multivariate logistic regression analysis. The results showed that AVS (OR = 4.52, 95%CI: 1.79–11.41, *P* = 0.001) and histological grade (OR = 0.04, 95%CI: 0.01–0.18, *P* < 0.001) were identified as independent predictors, leading to the construction of the CPA model. BPS, tumor size, and histological grade were included in the multivariate logistic regression analysis. The results showed that BPS (1 vs. 2: OR = 0.26, 95%CI: 0.10–0.67, *P* = 0.005; 1 vs. 3: OR = 0.12, 95%CI: 0.03–0.41, *P* < 0.001; 1 vs. 4: OR = 0.40, 95%CI: 0.03–3.00, *P* = 0.374; and 1 vs. 5: OR = 0.22, CI: 0.01–3.86, *P* = 0.303) and histological grade (OR = 0.04, 95%CI: 0.01–18, *P* < 0.001) were identified as independent predictors, leading to the construction of the CPP model. The DeLong test showed that the AUC of the CPP model (0.816) was higher than that of the CPF (0.778) and CPA (0.806) models (Table 3; Fig. 5).

Discussion

The results of our study revealed a positive correlation between breast peritumor score and invasive clinicopathological characteristics in M-IDC. Furthermore, BPS 1 MRI peritumoral characteristics without FBE or AVS were closely associated with luminal A-like breast cancer. Meanwhile, an elevated BPS was associated with larger tumors and a higher histologic grade.

Advances in medical technology have led to continuous improvements in comprehensive individualized treatment of breast cancer by combining neoadjuvant therapy with surgical treatment. Consequently, there is an increasing demand for accurate diagnosis, staging, molecular typing, and efficacy evaluation of breast cancer [15]. The markers of invasive breast cancer include tumor size, histological grade, lymphovascular invasion, axillary lymph node metastasis, Ki-67 index, and ER and HER2 expression. These indicators serve as crucial references for further clinical intervention and prognostic evaluation. Pathologists determine the histological grade by evaluating three parameters of invasive breast

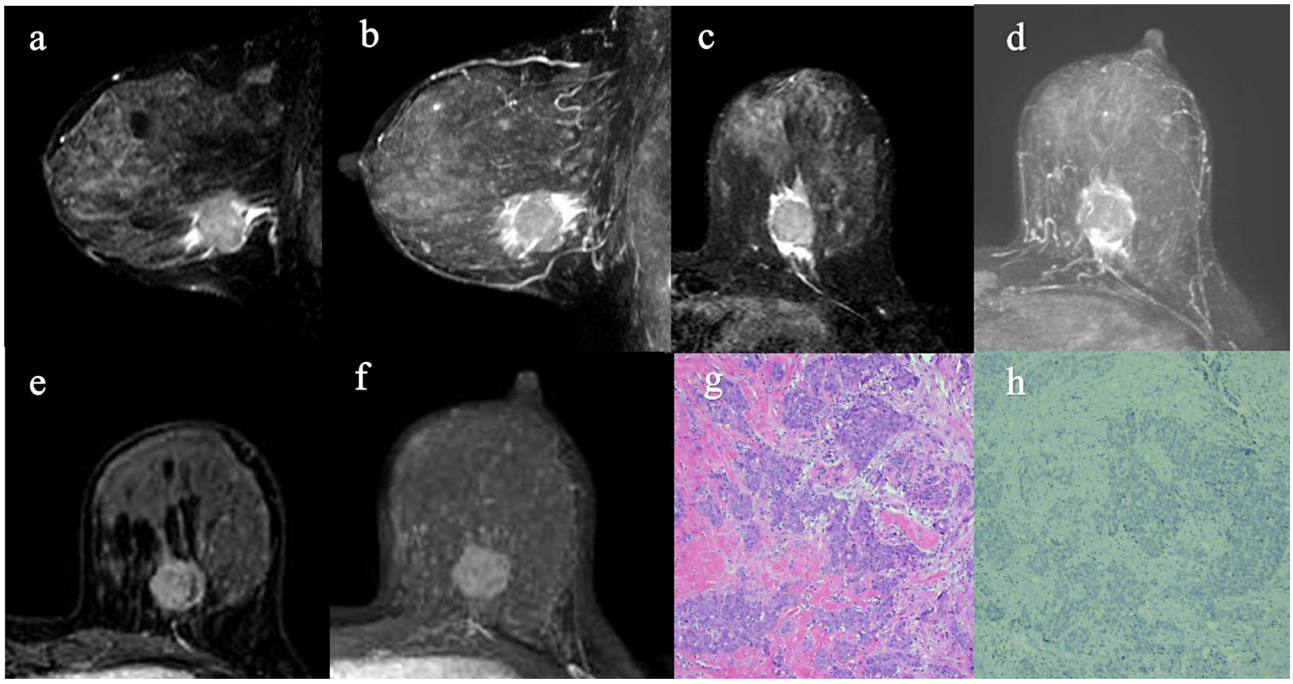

Fig. 3 A grade III triple-negative invasive ductal carcinoma in the left inner lower breast quadrant, 2.5 × 2.1 × 1.5 cm3 in size, no lymphovascular invasion, negative incisal margin, and no metastasis in sentinel lymph nodes. Preoperative MRI showed a mass in left inferior internal breast quadrant, demonstrating isointense signals and focal breast edema(peritumoral edema and prepectoral edema) on T2W-SPAIR images (a-d), with positive adjacent vascular signs on EDCE and MIP images (e, f). Postoperative pathology showed: invasive ductal carcinoma(HE staining ×100, g) and ER negative (immunohistochemistry staining ×100, h) in tumor cells amplified by EnVision method, the source of antibody: Gene Tech (Shanghai) Conpany Limited

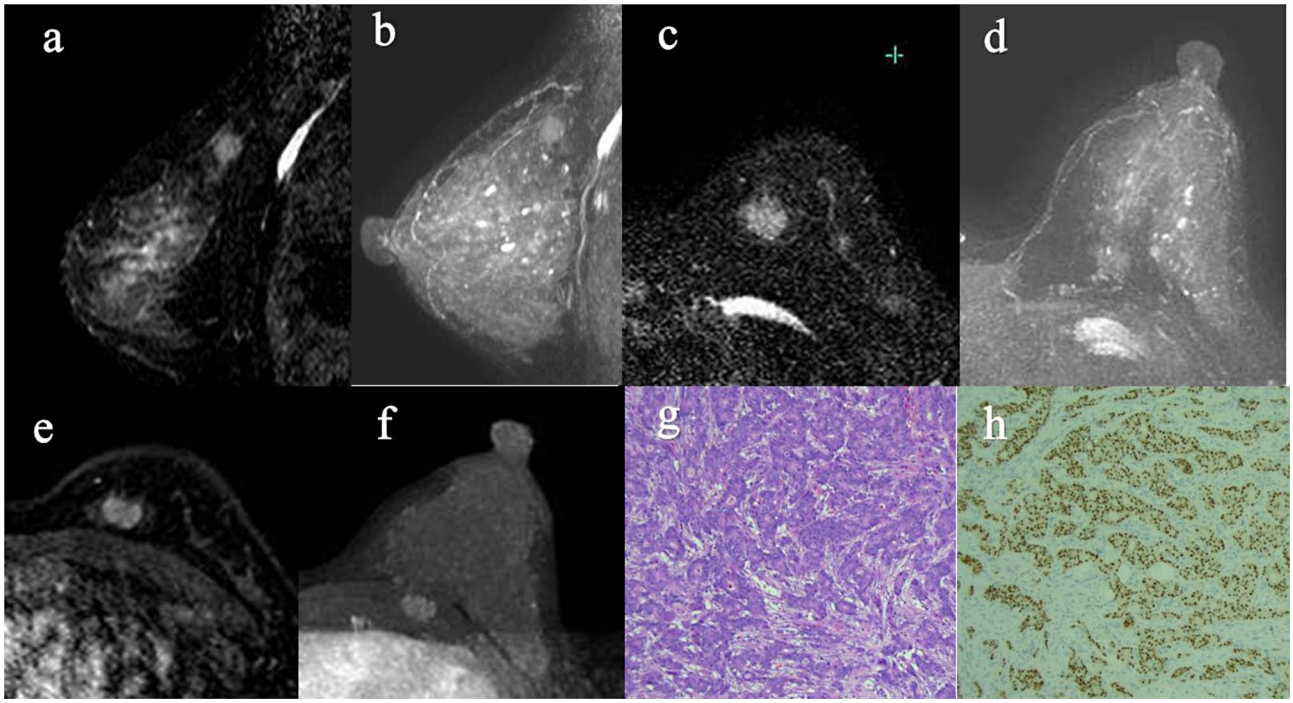

Fig. 4 A grade II invasive ductal carcinoma of the left breast, Lumina A type, 1.1 × 0.8 × 0.6 cm3 in size, no lymphovascular invasion, negative incisal margin, and no metastasis in sentinel lymph nodes. Preoperative MRI showed a mass in the upper quadrant of the left internal breast, demonstrating isointense signals and no focal edema on T2W-SPAIR images (a-d), with absence of adjacent vascular signs on EDCE and MIP images (e, f). Postoperative pathology showed: invasive ductal carcinoma (HE staining ×100, g), and ER strongly positive (immunohistochemistry staining ×100, h) in tumor cells amplified by EnVision method, the source of antibody: Gene Tech (Shanghai) Conpany Limited

Table 3 Comparison of prediction performance of three models

model	AUC (95%CI)	Z	*P* value (vs. CPP)
CPP	0.816 (0.759–0.873)	-	-
CPA	0.806 (0.745–0.867)	Z=-0.420	0.674
CPF	0.778 (0.719–0.837)	Z=-2.073	**0.038**

Statistically significant *p*-values are bolded

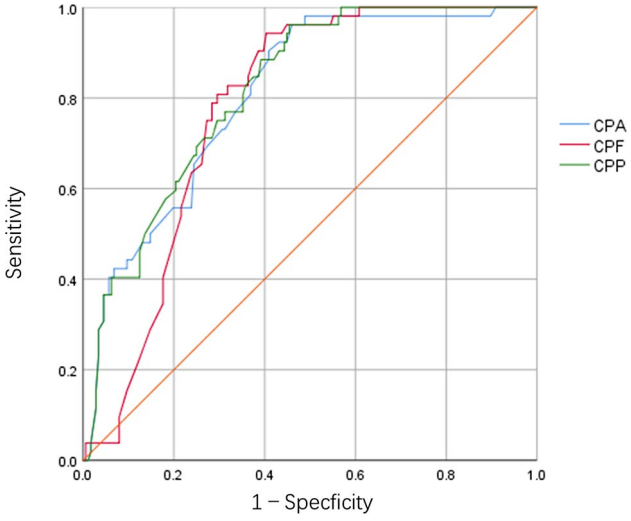

Fig. 5 The ROC curves of three models

cancer: crypt formation, nuclear pleomorphism, and mitotic count. It is a direct manifestation of the degree of tumor malignancy and has important guiding significance for clinical prediction of the prognosis of invasive breast cancer [16]. The presence of lymphovascular invasion in breast cancer signifies the development of a tumor thrombus within the lymphatic vessels and vascular system surrounding the lesion. This pathway serves as a crucial route for tumor metastasis through blood vessels and is associated with decreased long-term survival and increased recurrence rates [17]. Axillary lymph node metastasis, the most common route of metastasis in invasive breast cancer, is closely associated with a poor prognosis. It is a key determinant in treatment planning and prognosis [18]. The Ki-67 index, a marker of cell proliferation, exhibits a significant positive correlation with tumor malignancy. Moreover, it plays a crucial role in determining treatment strategies for invasive breast cancer [19]. The expressions of ER and HER2 play a pivotal role in predicting the prognosis of invasive breast cancer because they are crucial factors for endocrine therapy and targeted anti-HER2 therapy [20, 21].

In our study, we observed a significant association between BPS and larger tumor size, higher histologic grade, positive LVI, positive ALN metastasis, negative ER status, and a higher Ki-67 index in patients with M-IDC. Cheon et al. [22] conducted a study with 353 patients with breast cancer who underwent radical surgery and identified N stage, lymphovascular invasion, and peritumoral edema as independent risk factors for local recurrence and distant metastasis of invasive breast cancer within five years. Other studies have consistently demonstrated that patients with invasive breast cancer older, have a higher histological grade, exhibit positive lymphatic vascular invasion and axillary lymph node metastasis, express HER2 positively, lack ER expression, and display a high Ki-67 index are more likely to present with positive signs of FBE [23, 24]. However, many early studies failed to accurately define the indicators of FBE, and the majority did not categorize them [25]. Additionally, extensive research has consistently demonstrated the pivotal role of angiogenesis in tumor growth and metastasis, with AVS serving as a key indicator for assessing the malignancy of breast tumors [11]. In 2021, Harada et al. [10] initially established and employed the breast edema score (BES) to classify breast edema. Their study revealed a positive correlation between the BES grade and both progression-free survival and overall survival rates within ten years of multidisciplinary treatment for invasive breast cancer. Furthermore, high BES values (indicating prepectoral edema) may serve as an early symptom of inflammatory breast cancer. Our study demonstrated a significant and positive association between higher levels of BPS (prepectoral edema and subcutaneous edema) and indicators of high breast cancer aggressiveness, including tumor size larger than 3 cm, histologic grade III, positive LVI, positive ALN metastasis, negative ER status, and a higher Ki-67 index in patients with M-IDC.Other studies have indicated a positive correlation between BES and the biological aggressiveness of tumors, suggesting that higher BES levels are associated with poorer prognosis [26, 27]. Xu et al. [28] reported a significant positive correlation between BES and clinicopathological factors of biological invasiveness, suggesting that the absence of FBE and peritumoral edema may be indicative of a low burden of lymph node metastasis (less than three pathologically confirmed positive lymph node metastases). Conversely, high-grade FBE (prethoracic edema and subcutaneous edema) may be associated with a high burden of lymph node metastasis (more than or equal to three pathologically confirmed positive lymph node metastases). We established the BPS to validate the value of the BES and address the limitations of relying solely on the BES and AVS, thereby enhancing the accuracy of detecting peritumoral features on breast MRI.

Surprisingly, all FBE-positive cases were AVS-positive, suggesting that there was a causal relationship between the emergence of neovascularization and the formation of FBE. These results corroborate the findings of previous

studies, indicating that newly formed vessels exhibit diminished robustness owing to an incomplete vascular structure and abnormal lymphatic drainage [29]. The consequent vascular leakage and subsequent cytokine release ultimately lead to fluid accumulation within the breast tissues [30]. Our findings indicate that AVS may underlie the manifestation of FBE, thereby establishing a close association among FBE, robust tumor vascularization, and rapid proliferation. Additionally, our study demonstrated a significant correlation between tumor size and BPS in patients with M-IDC, with larger tumors exhibiting higher BPS levels. These findings support the notion that large space-occupying tumors tend to elicit a mass effect, leading to mechanical obstruction in the surrounding area and resulting in FBE [25].

This study found that a higher BPS grade was associated with a higher histological grade and Ki-67 index, indicating higher malignancy, greater tumor neovascularization, and a greater probability of breast interstitial edema. Both the histological grade and Ki-67 index are direct manifestations of tumor proliferation and are essential reference indices for clinical prognosis prediction and multidisciplinary treatment decision-making [31, 32]. In addition, our study showed that a higher BPS grade was associated with a higher rate of lymphovascular invasion. When cancer cells invade or block the trunk of the lymphatic vascular system, the collateral system transitions to the main lymphatic drainage route and prepectoral edema may develop because cancer cells further block or invade the vasculature posterior to the breast. Subcutaneous edema may be caused by tumor emboli blocking the distant skin and subskin lymphatic vascular system, resulting in edema and thickening of the skin and subskin tissues, indicating advanced cancer [33]. Our study also found that the higher the BPS score, the higher the probability of positive axillary lymph node metastasis. Several studies have confirmed that focal edema is independently associated with axillary lymph node metastasis, and the higher the grade of edema, the greater the burden of lymph node metastasis [34, 35]. Therefore, high BPS levels are significantly and positively correlated with highly aggressive pathological biomarkers, and play a crucial role in predicting disease recurrence, metastasis, and long-term prognosis.

Invasive breast cancer is highly heterogeneous and different molecular subtypes have significantly different treatment methods, efficacies, and clinical prognoses [36]. Among all molecular subtypes, luminal A-like breast cancer has the highest incidence, a relatively low degree of malignancy, mainly endocrine therapy, and a relatively good prognosis. With the advent of anti-HER2 targeted drugs, prognosis has greatly improved [37]. However, triple-negative breast cancer is the most malignant and lethal subtype, prone to recurrence and metastasis [38]. Our findings indicate that luminal A-like tumors are more likely to present with smaller tumor sizes, lower histological grades, and lesions with BPS 1 features. However, patients with triple-negative and HER2-positive M-IDC tended to have larger tumors, higher histological grades, and more frequent FBE and AVS. Many previous studies have confirmed that non-breast focal edema is more closely related to luminal A-like breast cancer [39, 40], whereas prepectoral and subcutaneous edema are more common in triple-negative and HER2-positive breast cancer [41, 42]. A comparison of the diagnostic efficacy of the different models for luminal A-like breast cancer confirmed that the CPP model had the best diagnostic performance. Therefore, BPS can more accurately reflect the biological aggressiveness of breast cancer and is a potentially valuable non-invasive imaging biomarker.

This study had several limitations. Firstly, despite implementing observer agreement assessments to evaluate AVS and FBE, subjective evaluations may have introduced inherent variability. Secondly, non-mass enhancements, many confirmed as lesions expressing HER2, were excluded from our analysis because of the inherent composition of interspersed fatty tissue and normal fibroglandular areas, which could potentially affect the accuracy of the measurements. The exclusion of non-mass enhancements contributed to the small number of HER2-positive cases. Thirdly, the single-center retrospective study had an insufficient total number of cases, and some groups had a small number of cases. Fourthly, we excluded cases with preoperative biopsies or neoadjuvant therapy, resulting in a limited number of cases in the BPS4,5 group.

In conclusion, BPS has the potential to serve as a valuable biomarker for assessing the aggressiveness of breast cancer. We anticipate further multicenter and prospective studies utilizing artificial intelligence methods to delve deeper into peritumoral features.

Acknowledgements
Not applicable.

Author contributions
J. H.: Writing – original draft, Methodology, Conceptualization, Data curation. J. K.: Writing – original draft, Methodology, Conceptualization, Data curation.S. X.: Writing - review & editing, Investigation, Methodology. L.P.: Writing - review & editing, Conceptualization. L. C.: Writing - review & editing, Project administration, Resources. H. Z.:: Writing - review & editing, Project administration, Resources.X. Z.: Writing - review & editing, Project administration, Resources.

Funding
There was no external funding for this study itself. All authors had full access to all of the data in this study and take complete responsibility for the integrity of the data and accuracy of the data analysis.

Data availability
The datasets analyzed during the current study are available from the corresponding author on reasonable request.

Declarations

Ethics approval and consent to participate

This retrospective study was approved by the Ethics Committee of Quzhou People's Hospital and the informed consent requirement was waived (No. AF/SW-05/01.0-2023-045).

Consent for publication

Not applicable.

Competing interests

The authors declare no competing interests.

Abbreviations

AVS, adjacent vessel sign; ALN, axillary lymph node.
BES, breast edema score.
BPS, breast peritumor score.
EDCE, early dynamic contrast-enhanced.
ER, estrogen receptor.
CPA, clinicopathological-AVS.
CPF, clinicopathological-FBE.
CPP, clinicopathological-BPS.
FBE, focal breast edema.
LVI, lymphovascular invasion.
M-IDC, mass-type invasive ductal carcinoma.
MIP, maximum intensity projection.
T1WI, T1-weighted.
T2WI, T2-weighted sequence.

Received: 5 August 2024 / Accepted: 26 November 2024
Published online: 05 December 2024

References

1. Sung H, Ferlay J, Siegel RL, Laversanne M, Soerjomataram I, Jemal A, et al. Global Cancer statistics 2020: GLOBOCAN estimates of incidence and Mortality Worldwide for 36 cancers in 185 countries. CA Cancer J Clin. 2021;71:209–49. https://doi.org/10.3322/caac.21660.
2. Mann RM, Cho N, Moy L, Breast MRI. State of the art. Radiology. 2019;292:520–36. https://doi.org/10.1148/radiol.2019182947.
3. Kim S-Y, Cho N, Hong H, Lee Y, Yoen H, Kim YS, et al. Abbreviated screening MRI for women with a history of breast Cancer: comparison with full-protocol breast MRI. Radiology. 2022;305:36–45. https://doi.org/10.1148/radiol.213310.
4. Kwon M-R, Choi JS, Won H, Ko EY, Ko ES, Park KW, et al. Breast Cancer screening with abbreviated breast MRI: 3-year Outcome Analysis. Radiology. 2021;299:73–83. https://doi.org/10.1148/radiol.2021202927.
5. Wu J, Sun X, Wang J, Cui Y, Kato F, Shirato H, et al. Identifying relations between imaging phenotypes and molecular subtypes of breast cancer: Model discovery and external validation. J Magn Reson Imaging. 2017;46:1017–27. https://doi.org/10.1002/jmri.25661.
6. Braman NM, Etesami M, Prasanna P, Dubchuk C, Gilmore H, Tiwari P, et al. Intratumoral and peritumoral radiomics for the pretreatment prediction of pathological complete response to neoadjuvant chemotherapy based on breast DCE-MRI. Breast Cancer Res. 2017;19:57. https://doi.org/10.1186/s13058-017-0846-1.
7. Santucci D, Faiella E, Cordelli E, Calabrese A, Landi R, de Felice C, et al. The impact of Tumor Edema on T2-Weighted 3T-MRI invasive breast Cancer histological characterization: a pilot Radiomics Study. Cancers (Basel). 2021;13. https://doi.org/10.3390/cancers13184635.
8. Uematsu T. Focal breast edema associated with malignancy on T2-weighted images of breast MRI: peritumoral edema, prepectoral edema, and subcutaneous edema. Breast Cancer. 2015;22:66–70. https://doi.org/10.1007/s12282-014-0572-9.
9. Jirarayapong J, Portnow LH, Chikarmane SA, Lan Z, Gombos EC. High Peritumoral and Intratumoral T2 Signal Intensity in HER2-Positive breast cancers on preneoadjuvant breast MRI: Assessment of associations with histopathologic characteristics. AJR Am J Roentgenol. 2024;222:e2330280. https://doi.org/10.2214/AJR.23.30280.
10. Harada TL, Uematsu T, Nakashima K, Kawabata T, Nishimura S, Takahashi K, et al. Evaluation of breast edema findings at T2-weighted breast MRI is useful for diagnosing Occult inflammatory breast Cancer and can predict prognosis after Neoadjuvant Chemotherapy. Radiology. 2021;299:53–62. https://doi.org/10.1148/radiol.2021202604.
11. Han M, Kim TH, Kang DK, Kim KS, Yim H. Prognostic role of MRI enhancement features in patients with breast cancer: value of adjacent vessel sign and increased ipsilateral whole-breast vascularity. AJR Am J Roentgenol. 2012;199:921–8. https://doi.org/10.2214/AJR.11.7895.
12. Çetinkaya E, Yıldız Ş, Otçu H, Sharifov R, Çelik Yabul F, Alkan A. The value of adjacent vessel sign in malignant breast tumors. Diagn Interv Radiol. 2022;28:463–9. https://doi.org/10.5152/dir.2022.211228.
13. Choi JS. Advantages and Limitations]. J Korean Soc Radiol. 2023;84:3–14. https://doi.org/10.3348/jksr.2022.0142. [Breast Imaging Reporting and Data System (BI-RADS).
14. Lebeau A. [Updated WHO classification of tumors of the breast]. Pathologe. 2021;42:155–9. https://doi.org/10.1007/s00292-021-01019-3.
15. Papakonstantinou A, Gonzalez NS, Pimentel I, Suñol A, Zamora E, Ortiz C, et al. Prognostic value of ctDNA detection in patients with early breast cancer undergoing neoadjuvant therapy: a systematic review and meta-analysis. Cancer Treat Rev. 2022;104:102362. https://doi.org/10.1016/j.ctrv.2022.102362.
16. Wang Y, Acs B, Robertson S, Liu B, Solorzano L, Wählby C, et al. Improved breast cancer histological grading using deep learning. Ann Oncol. 2022;33:89–98. https://doi.org/10.1016/j.annonc.2021.09.007.
17. Zhong Y-M, Tong F, Shen J. Lympho-vascular invasion impacts the prognosis in breast-conserving surgery: a systematic review and meta-analysis. BMC Cancer. 2022;22:102. https://doi.org/10.1186/s12885-022-09193-0.
18. Lai J, Chen Z, Liu J, Zhu C, Huang H, Yi Y, et al. A Radiogenomic multimodal and whole-transcriptome sequencing for preoperative prediction of axillary lymph node metastasis and drug therapeutic response in breast cancer: a retrospective, machine learning and international multi-cohort study. Int J Surg. 2024;110:2162–77. https://doi.org/10.1097/JS9.0000000000001082.
19. Smith I, Robertson J, Kilburn L, Wilcox M, Evans A, Holcombe C, et al. Long-term outcome and prognostic value of Ki67 after perioperative endocrine therapy in postmenopausal women with hormone-sensitive early breast cancer (POETIC): an open-label, multicentre, parallel-group, randomised, phase 3 trial. Lancet Oncol. 2020;21:1443–54. https://doi.org/10.1016/S1470-2045(20)30458-7.
20. Ji Y, Whitney HM, Li H, Liu P, Giger ML, Zhang X. Differences in Molecular Subtype Reference standards Impact AI-based breast Cancer classification with dynamic contrast-enhanced MRI. Radiology. 2023;307:e220984. https://doi.org/10.1148/radiol.220984.
21. Palmieri C, Linden H, Birrell SN, Wheelwright S, Lim E, Schwartzberg LS, et al. Activity and safety of enobosarm, a novel, oral, selective androgen receptor modulator, in androgen receptor-positive, oestrogen receptor-positive, and HER2-negative advanced breast cancer (study G200802): a randomised, open-label, multicentre, multinational, parallel design, phase 2 trial. Lancet Oncol. 2024;25:317–25. https://doi.org/10.1016/S1470-2045(24)00004-4.
22. Cheon H, Kim HJ, Kim TH, Ryeom H-K, Lee J, Kim GC, et al. Invasive breast Cancer: Prognostic Value of Peritumoral Edema identified at preoperative MR Imaging. Radiology. 2018;287:68–75. https://doi.org/10.1148/radiol.2017171157.
23. Sung P, Lee JY, Cheun J-H, Choi IS, Park JH, Park JH, et al. Prognostic implication of focal breast edema on preoperative breast magnetic resonance imaging in breast Cancer patients. J Breast Cancer. 2023;26:479–91. https://doi.org/10.4048/jbc.2023.26.e35.
24. Huang Z, Tu X, Lin Q, Zhan Z, Tang L, Liu J, et al. Intramammary edema of invasive breast cancers on MRI T(2)-weighted fat suppression sequence: correlation with molecular subtypes and clinical-pathologic prognostic factors. Clin Imaging. 2022;83:87–92. https://doi.org/10.1016/j.clinimag.2021.12.023.
25. Park NJ-Y, Jeong JY, Park JY, Kim HJ, Park CS, Lee J, et al. Peritumoral edema in breast cancer at preoperative MRI: an interpretative study with histopathological review toward understanding tumor microenvironment. Sci Rep. 2021;11:12992. https://doi.org/10.1038/s41598-021-92283-z.
26. Chen Y, Wang L, Luo R, Liu H, Zhang Y, Wang D. Focal breast edema and breast edema score on T2-weighted images provides valuable biological information for invasive breast cancer. Insights Imaging. 2023;14:73. https://doi.org/10.1186/s13244-023-01424-7.
27. Cakir Pekoz B, Dilek O, Koseci T, Tas ZA, Irkorucu O, Gulek B. Can peritumoral edema evaluated by magnetic resonance imaging before neoadjuvant chemotherapy predict complete pathological response in breast cancer? Scott Med J. 2023;68:121–8. https://doi.org/10.1177/00369330231174230.
28. Xu Z, Ding Y, Zhao K, Han C, Shi Z, Cui Y, et al. MRI characteristics of breast edema for assessing axillary lymph node burden in early-stage breast cancer:

a retrospective bicentric study. Eur Radiol. 2022;32:8213–25. https://doi.org/10.1007/s00330-022-08896-z.
29. Hester RH, Hortobagyi GN, Lim B. Inflammatory breast cancer: early recognition and diagnosis is critical. Am J Obstet Gynecol. 2021;225:392–6. https://doi.org/10.1016/j.ajog.2021.04.217.
30. Harada TL, Uematsu T, Nakashima K, Sugino T, Nishimura S, Takahashi K, et al. Is the presence of edema and necrosis on T2WI pretreatment breast MRI the key to predict pCR of triple negative breast cancer? Eur Radiol. 2020;30:3363–70. https://doi.org/10.1007/s00330-020-06662-7.
31. Yang Z-G, Ren L-H, Wang F, Wang P-L, Wang W-Y, Lin S-Y. Ki-67 change in Anthracyline-containing Neoadjuvant Chemotherapy response in breast Cancer. Curr Med Sci. 2024;44:156–67. https://doi.org/10.1007/s11596-023-2824-4.
32. Kurozumi S, Seki N, Narusawa E, Honda C, Tokuda S, Nakazawa Y, et al. Identification of MicroRNAs Associated with histological Grade in early-stage invasive breast Cancer. Int J Mol Sci. 2023;25. https://doi.org/10.3390/ijms25010035.
33. Uematsu T, Kasami M, Watanabe J. Is evaluation of the presence of prepectoral edema on T2-weighted with fat-suppression 3 T breast MRI a simple and readily available noninvasive technique for estimation of prognosis in patients with breast cancer? Breast Cancer. 2014;21:684–92. https://doi.org/10.1007/s12282-013-0440-z.
34. Byon JH, Park YV, Yoon JH, Moon HJ, Kim E-K, Kim MJ, et al. Added value of MRI for invasive breast Cancer including the entire axilla for evaluation of high-level or Advanced Axillary Lymph Node Metastasis in the Post-ACOSOG Z0011 trial era. Radiology. 2021;300:46–54. https://doi.org/10.1148/radiol.2021202683.
35. Song SE, Woo OH, Cho Y, Cho KR, Park KH, Kim JW. Prediction of Axillary Lymph Node Metastasis in early-stage triple-negative breast Cancer using Multiparametric and Radiomic features of breast MRI. Acad Radiol. 2023;30(Suppl 2):S25–37. https://doi.org/10.1016/j.acra.2023.05.025.
36. Bodewes FTH, van Asselt AA, Dorrius MD, Greuter MJW, de Bock GH. Mammographic breast density and the risk of breast cancer: a systematic review and meta-analysis. Breast. 2022;66:62–8. https://doi.org/10.1016/j.breast.2022.09.007.
37. Nitz U, Gluz O, Graeser M, Christgen M, Kuemmel S, Grischke E-M, et al. De-escalated neoadjuvant pertuzumab plus trastuzumab therapy with or without weekly paclitaxel in HER2-positive, hormone receptor-negative, early breast cancer (WSG-ADAPT-HER2+/HR-): survival outcomes from a multicentre, open-label, randomised, phase 2 trial. Lancet Oncol. 2022;23:625–35. https://doi.org/10.1016/S1470-2045(22)00159-0.
38. Leon-Ferre RA, Goetz MP. Advances in systemic therapies for triple negative breast cancer. BMJ. 2023;381:e071674. https://doi.org/10.1136/bmj-2022-071674.
39. Net JM, Whitman GJ, Morris E, Brandt KR, Burnside ES, Giger ML, et al. Relationships between Human-extracted MRI tumor phenotypes of breast Cancer and clinical prognostic indicators including receptor status and molecular subtype. Curr Probl Diagn Radiol. 2019;48:467–72. https://doi.org/10.1067/j.cpradiol.2018.08.003.
40. Panzironi G, Moffa G, Galati F, Marzocca F, Rizzo V, Pediconi F. Peritumoral edema as a biomarker of the aggressiveness of breast cancer: results of a retrospective study on a 3 T scanner. Breast Cancer Res Treat. 2020;181:53–60. https://doi.org/10.1007/s10549-020-05592-8.
41. Liang T, Hu B, Du H, Zhang Y. Predictive value of T2-weighted magnetic resonance imaging for the prognosis of patients with mass-type breast cancer with peritumoral edema. Oncol Lett. 2020;20:314. https://doi.org/10.3892/ol.2020.12177.
42. Moradi B, Gity M, Etesam F, Borhani A, Ahmadinejad N, Kazemi MA. Correlation of apparent diffusion coefficient values and peritumoral edema with pathologic biomarkers in patients with breast cancer. Clin Imaging. 2020;68:242–8. https://doi.org/10.1016/j.clinimag.2020.08.020.

Publisher's note